Heating Characteristics of Array Applicator Composed of Two Coaxial-Slot Antennas for Microwave Coagulation Therapy

Kazuyuki Saito, *Student Member, IEEE,* Yoshihiko Hayashi, Hiroyuki Yoshimura, *Member, IEEE,* and Koichi Ito, *Member, IEEE*

***Abstract*—Microwave coagulation therapy (MCT) has been used mainly for the treatment of small-size tumors. The operating frequency is 2450 MHz for the present MCT. In conventional MCT antennas, there exists a problem that the size of the coagulated region is insufficient. In this paper, we analyzed the heating characteristics of an array applicator composed of two coaxial-slot antennas by using computer simulation. The validity of the analysis was confirmed by the experiment using the liver of a pig. Moreover, we investigated the relation between the array spacing and heating volume produced by the two-antenna array applicator. As a result, the coagulated region required in the MCT could almost be achieved under the conditions that the net input power of each antenna was 50 W and the array spacing was 10 mm.**

***Index Terms*—Array applicator, FDTD method, microwave coagulation therapy, temperature distribution.**

I. Introduction

MICROWAVE coagulation therapy (MCT) has been used mainly for the treatment of hepatocellular carcinoma [1], [2]. In the treatment, a thin microwave antenna is inserted into the tumor, and the microwave energy provided by the antenna heats up the tumor to produce the coagulated region including the cancer cells. The input power of the antenna is several tens of watts. We have to heat the cancer cells up to at least 60 °C for a few minutes or longer.

There are currently two major problems that need to be improved for conventional MCT antennas. First, in the conventional MCT antenna, the coagulated tissue adheres to the antenna because the conductor contacts with the coagulated tissue directly. Second, the size of the coagulated region is insufficient, especially in the perpendicular direction of the antenna axis. It has been desired from the clinical side that the coagulated region becomes a sphere of about 3 cm in diameter. The first problem can be solved by inserting the antenna into a catheter. However, it is difficult to solve the second problem by using one antenna.

Until now, the intercept of the blood flow in the liver has been investigated to expand the coagulated region, though the structure of the applicator has not been theoretically improved [3]. The authors have studied the heating characteristics of one coaxial-slot antenna for the MCT [4]. However, we have not yet obtained the method that satisfies the sufficient coagulated region in the perpendicular direction of the antenna.

In this paper, to expand the coagulated region, we have studied the heating characteristics of an array applicator composed of coaxial-slot antennas with a catheter by using the computer simulation. As a basic study of an array applicator for the MCT, we introduced the two-antenna array applicator, which is the simplest structure.

In Section II, we describe the structure of the coaxial-slot antenna. In Section III, the procedure for computer simulation to obtain the temperature distribution around the antenna inside the biological tissue is described. In Section IV, we confirm the validity of our analysis by comparing the calculated results with experimental results. In Section V, we evaluate the heating performances of a two-antenna array applicator by introducing three indexes. In particular, the relations between the array spacing and these indexes are shown. Finally, conclusions are presented in Section VI.

II. Coaxial-Slot Antenna

Fig. 1 and Table I show the configuration and parameters of the coaxial-slot antenna [5], respectively. Here, d_b is the diameter of the antenna, d_c is the external diameter of the catheter, t_c is the thickness of the catheter, L_{ts} is the length from the tip to the center of the slot, and D_t is the insertion depth. We used a thin semirigid coaxial cable with a diameter of 1.19 mm because the thin antenna is required in the interstitial treatments. A ring slot is cut on the outer conductor and the tip of the cable is short circuited. We can control the heating pattern along the antenna axis by changing the position, number, and width of the slots. In this paper, however, we considered only one-slot antenna whose slot width W_{sl} is 1.0 mm to simplify the discussion. L_{ts} was set to 5 mm because the effective heating around the tip of the antenna is very important to the interstitial heating and because the electric field becomes strong near the slot. We inserted the antenna to the catheter made of PTFE for the hygiene so that we could prevent from adhering the coagulated tissue to the antenna. In addition, the operating frequency was set to 2450 MHz because the frequency is used for the conventional MCT.

III. Description of Analytical Model

In this section, we describe the method of the numerical analyses for the electric and temperature distributions inside

Manuscript received November 16, 1999; revised March 5, 2000.

K. Saito and Y. Hayashi are with the Graduate School of Science and Technology, Chiba University Faculty of Engineering, Chiba University, Chiba 263-8522, Japan (e-mail: saito@ap.tu.chiba-u.ac.jp)

H. Yoshimura and K. Ito are with the Department of Urban Environment Systems, Chiba 263-8522, Japan.

Publisher Item Identifier S 0018-9480(00)09530-2.

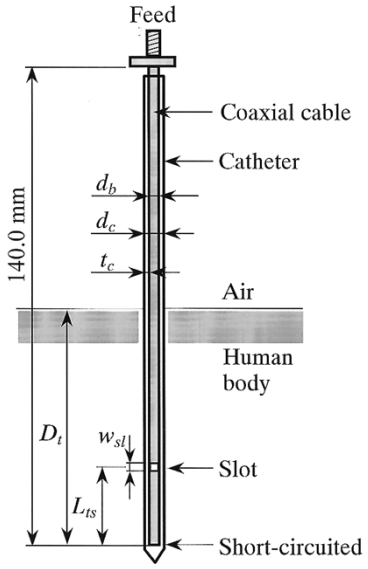

Fig. 1. Basic structure of the coaxial-slot antenna.

TABLE I
DIMENSIONS AND RELATIVE PERMITTIVITIES OF THE COAXIAL-SLOT ANTENNA

d_b (diameter of the antenna) [mm]	1.19
d_c (external diameter of the catheter) [mm]	1.79
t_c (thickness of the catheter) [mm]	0.3
L_{ts} (length from the tip to the center of the slot) [mm]	5.0
W_{sl} (width of the slot) [mm]	1.0
D_t (insertion depth) [mm]	70.0
ε_{ri} (relative permittivity of the inner dielectric)	2.03
ε_{rc} (relative permittivity of the catheter)	2.6

the biological tissue. First, we show the flowchart for computer simulation to obtain the temperature distribution around the antennas inside the tissue, the finite-difference time-domain (FDTD) analysis for the electromagnetic field is described, and finally, the temperature analysis by solving the bioheat transfer equation is explained.

A. Procedure for Analysis

Fig. 2 shows the flowchart of computer simulation for calculating the temperature distribution around the coaxial-slot antenna inside the tissue. First, we calculate the electric field around the antenna by using the FDTD method [6]. Next, we calculate the specific absorption rate (SAR) distribution around the antenna from

$$\mathrm{SAR} = \frac{\sigma}{\rho}|E|^2 \quad \mathrm{W/kg} \tag{1}$$

where σ is the conductivity of the tissue (S/m), ρ is the density of the tissue (kg/m^3), and E is the electric field (rms) (V/m). The SAR takes a value proportional to the square of the electric field around the antennas and is equivalent to the heating source generated by the electric field in the tissue.

Finally, in order to obtain the temperature distribution in the tissue, we numerically analyze the bioheat transfer equation including the obtained SAR distribution by using the finite-difference method (FDM).

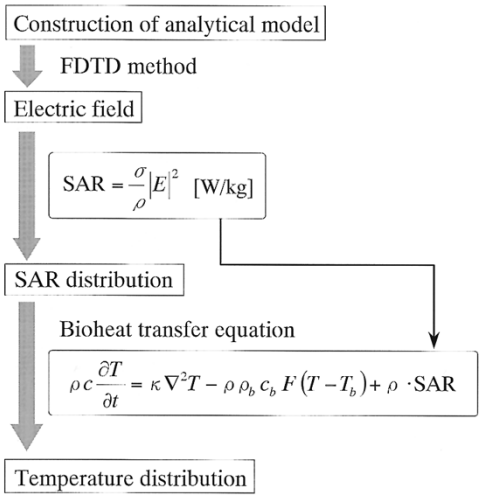

Fig. 2. Procedure for analysis of temperature distributions around antennas.

During the MCT, the electrical properties of the tissue change because this treatment generates a high-temperature region in the tissue to coagulate the cancer cells. The authors had already investigated this point [4]. From the result, we revealed the temperature dependence of the electrical properties of the tissue. In this paper, however, we used the fixed electric constants to simplify the calculation so that we could observe good agreement between the calculated and experimental results, as described in Section IV. Therefore, we assumed that the electric constants can be fixed in this problem.

B. FDTD Analysis for the Electromagnetic Field

Fig. 3 shows the FDTD analytical model. We employed a square model as the cross section of the antenna, as we had validated this model enough for practical use [7].

In the analysis, we employed the nonuniform grids and used small-size grids only for the antenna. The parameters used in the FDTD analysis are listed in Table II.

C. Temperature Analysis

We can calculate the temperature distribution inside the biological tissue by solving the bioheat transfer equation given by [8]

$$\rho c\frac{\partial T}{\partial t} = \kappa\nabla^2 T - \rho\rho_b c_b F(T-T_b) + \rho\cdot\mathrm{SAR} \tag{2}$$

where T is the temperature (°C), t is the time (s), ρ is the density (kg/m^3), c is the specific heat (J/kg·K), κ is the thermal conductivity (W/m·K), ρ_b is the density of the blood (kg/m^3), c_b is the specific heat of the blood (J/kg·K), T_b is the temperature of the blood (°C), and F is the blood flow rate (m^3/kg·s).

The first, second, and third terms in the right-hand side of (2) denote thermal conduction, heat dissipation by the blood flow, and heat generation by the electric field, respectively. In this paper, we assumed that the temperature of the blood T_b is equal to initial temperature of the tissue. We substitute the SAR obtained by the previous electromagnetic analysis into the

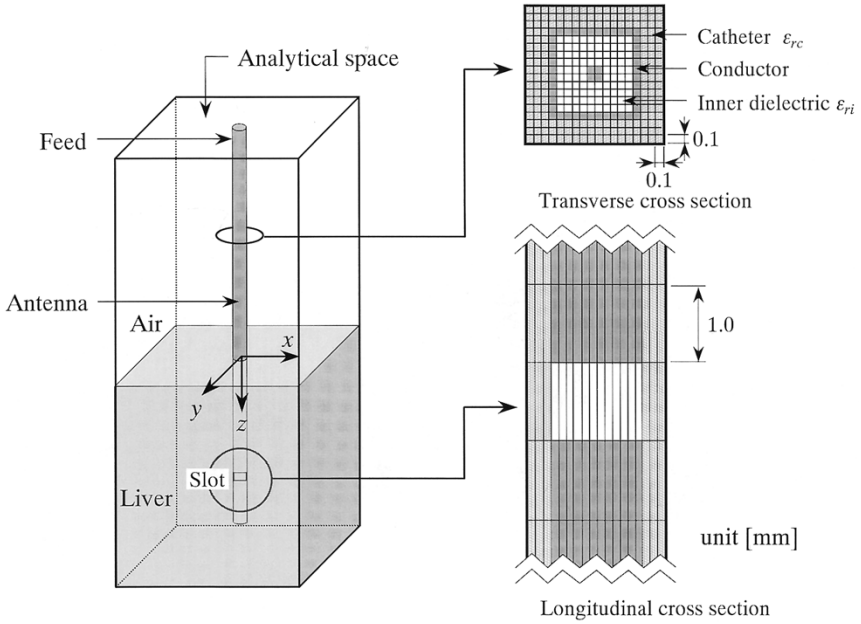

Fig. 3. FDTD analytical model of the coaxial-slot antenna.

TABLE II
PARAMETERS FOR FDTD ANALYSIS

Minimum cell size [mm]		
Δx	Δy	Δz
0.1	0.1	1.0
Time step [ps]		0.235
Absorbing boundary condition		Mur (1st order)

third term in the right-hand side of (2). The FDM was used in a numerical calculation for solving (2). The finite-difference approximation is shown in the Appendix. We employed the same grids as those of the electromagnetic analysis and only analyzed inside the tissue. In this case, the stability criterion of the temperature analysis was assumed to be (3) by referring to the paper by Wang *et al.* [9]

$$\Delta t \leq \frac{2\rho c}{\rho\rho_b c_b F + 4\kappa\left(\frac{1}{\Delta x^2}+\frac{1}{\Delta y^2}+\frac{1}{\Delta z^2}\right)} \tag{3}$$

where Δt (s) is the time step for temperature analysis and Δx, Δy, Δz (m) is the minimum cell sizes.

From (3), it is clear that we must choose a small time step when κ enlarges. In general, κ in the conductor of the antenna is very large compared with that in the biological tissue. However, we cannot choose a very small time step for the practical calculation. In this paper, we assumed that the heat transfer in the part of the conductor is small because the conductor part is a very small volume. Under this assumption, we replaced the antenna with an object having the same material as that of the catheter.

The results of temperature analysis in the interstitial applicator describe the fact that the very near region of the antenna becomes very high temperature. In this paper, we assumed that the maximum temperature in the analytical space is 100 °C because high temperature causes the evaporation of moisture in the tissue.

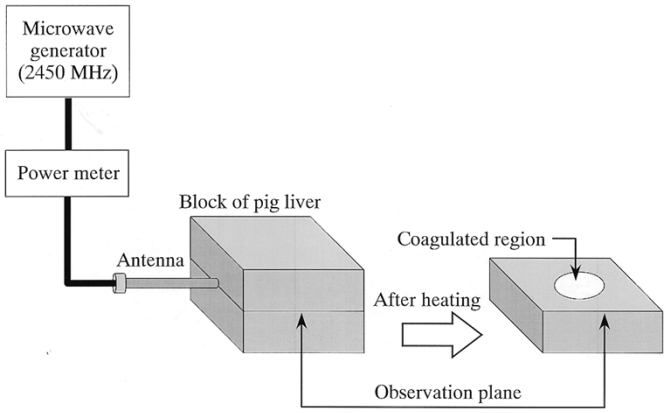

Fig. 4. Setup of coagulation experiment for validation of the analysis.

IV. VALIDATION OF ANALYSIS

A. Experimental System

Fig. 4 shows the setup of the coagulation experiment for validation of our analysis. We preheated the liver of a pig about 30 °C. Next, we placed the antenna into two liver blocks. In the coagulation experiment, we observed the net input power (input power minus reflection power) by using the power reflection meter (Rohde & Schwarz NRT, NRT-Z44). After heating, we observed the coagulated region on the surface of one piece of the liver block.

B. Analytical Condition

Fig. 5 and Table III show the analytical model and parameters for the analysis, respectively. (The parameters of the blood

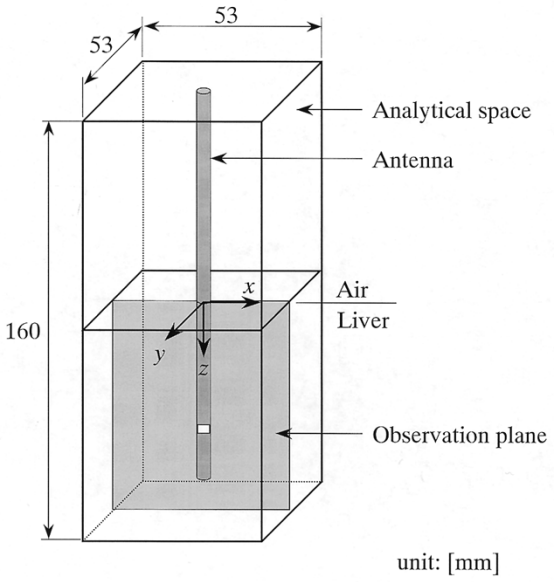

Fig. 5. Analytical space and observation plane.

TABLE III
ELECTRICAL AND THERMAL PROPERTIES OF THE MEDIA[1] [10]–[12]

	Liver	Antenna (catheter)
Relative permittivity	43.03	2.6
Conductivity [S/m]	1.69	——
Thermal conductivity [W/m·K]	0.5	0.272
Specific heat [J/kg·K]	3600	974
Density [kg/m^3]	1060	2200
Blood flow rate [m^3/kg·s]	5×10^{-6}	——
Density of the blood [kg/m^3]	1060	——
Specific heat of blood [J/kg·K]	3960	——

[1] [Online]. Available: http://www.fcc.gov/fcc-bin/dielec.sh

in Table III will be used in the following section.) Here, the parameters in Table III are the values of the human. However, we adopted the values of a liver of a pig for the following reasons.

We measured the relative permittivity and electrical conductivity of the liver of a pig by using the dielectric constant's measurement system (HP85070B), and obtained almost the same values as those of the human (Relative permittivity and conductivity of the liver of a pig are 43.66 and 1.73 S/m, respectively). From [10], the thermal conductivity of the liver of a human was from 0.467 to 0.527 and that of the liver of a pig was 0.528. Therefore, we adopted the value of 0.5 as the thermal conductivity of the livers of a pig and human. Moreover, we measured the density of the liver of a pig, and obtained almost the same value as that of the human.

From (3), for temperature analysis, we have to set the time step Δt smaller than 0.01899 s. Therefore, we adopted 0.01 s as Δt to satisfy the stability criterion enough. The coagulated region in the calculation was assumed to be 60 °C or more because the liver tissue begins to coagulate at 60 °C. Moreover, the antenna insertion depth D_t, net input power, and heating time were assumed to be 70 mm, 37.3 W, and 90 s, respectively.

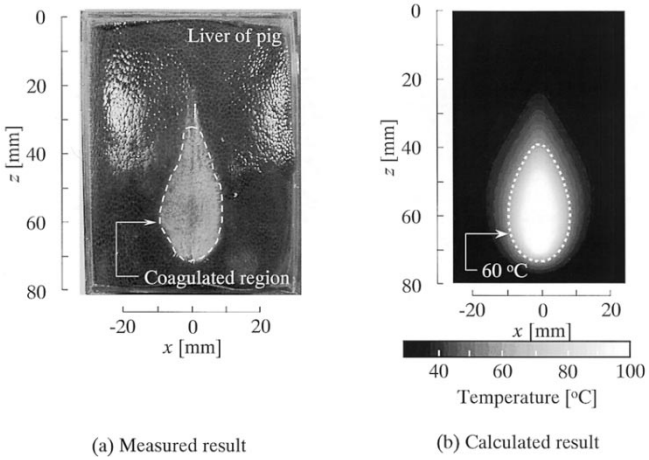

Fig. 6. Validation of analysis.

C. Results

Fig. 6(a) shows the result of coagulation experiment in the observation plane, and Fig. 6(b) shows the calculated result. In Fig. 6(a), a discolored region corresponds to a coagulated region, which became 60 °C or more under the experiment. In the experiment, the maximum sizes of the coagulated region of the x- and z-directions were 18.5 and 40.0 mm, respectively. In the calculation, the maximum sizes of coagulated region of the x- and z-directions were 18.5 and 37.0 mm, respectively. From the results, the size of coagulated region in the z-direction was approximately 10% different between the measured and calculated results. Moreover, the shape of coagulated region of the experiment was not slightly symmetric. It is considered that nonuniform contact of the antenna and the liver of a pig caused this result. However, we may say that good agreement is observed between the discolored region in the Fig. 6(a) and the region of 60 °C or more in Fig. 6(b).

V. EXPANSION OF COAGULATED REGION BY ARRAY APPLICATOR

In this section, we investigate the expansion of the coagulated region by using the two-antenna array applicator.

Fig. 7 shows the analytical space and observation planes for the two-antenna array applicator. Here, As denotes the array spacing. The observation plane 1 is the x–z plane at $y = 0$, the observation plane 2 is the x–y plane at $z = z_{\max}$ ($z_{\max}$ will be defined later) and observation plane 3 is the y–z plane at $x = 0$. We analyzed the coagulated region of the two-antenna array applicator with $As = 5, 10, 15, 20, 25$, or 30 mm, when the net input power of each antenna P_{net} was 25 or 50 W (The total net input power was 50 or 100 W.) In the MCT, the input power of one antenna is several tens of watts, therefore, we chose these values as the input power of one antenna. The initial temperature of the tissue, the heating time, and the antenna insertion depth were assumed to be 37 °C, 90 s, and 70 mm, respectively, by considering the situation of the actual treatment.

We evaluated the heating performances of the two-antenna array applicator by using the following indexes (see Fig. 8).

- *The length of the continuous area heated over 60 °C or more on the z-axis in observation plane 1*. We define this

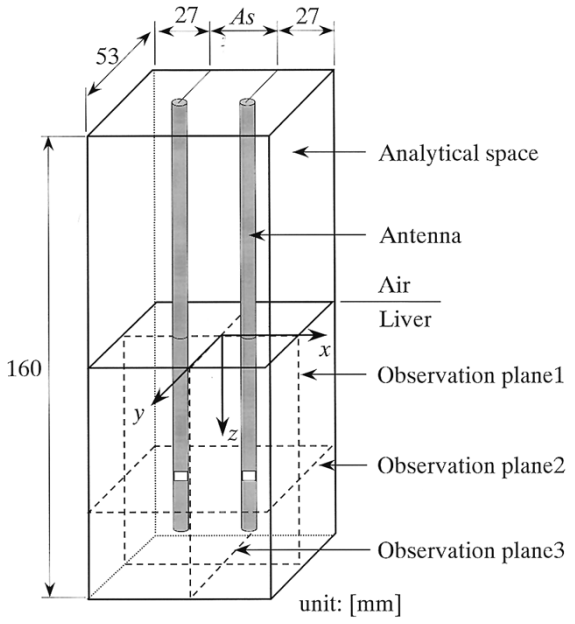

Fig. 7. Analytical space and observation planes for two-antenna array applicator.

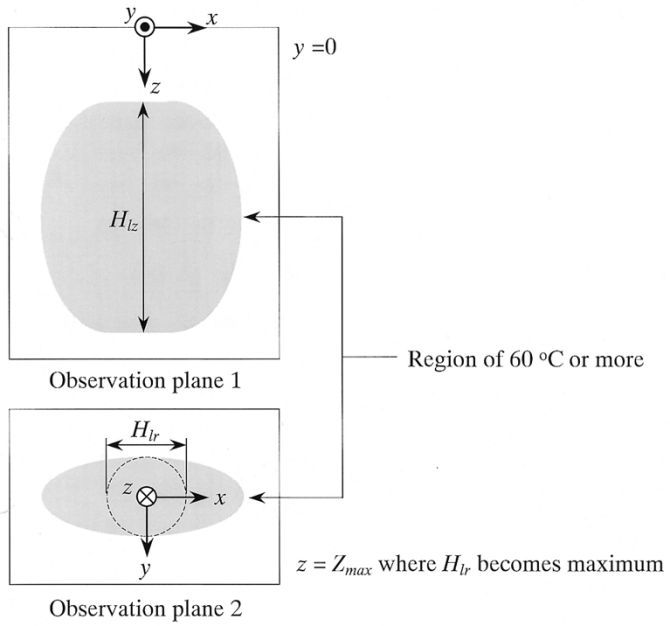

Fig. 8. Indexes for evaluating the heating performance of the two-antenna array applicator.

length as H_{lz}. When the array spacing As is sufficiently large and the region of 60 °C or more separates into two regions or more, $H_{lz} = 0$.

- *The maximum diameter of the continuous area heated over 60 °C or more in observation plane 2.* We define this diameter as H_{lr}. When the array spacing As is sufficiently large and the region of 60 °C or more separates into two regions or more, $H_{lr} = 0$.
- *The position of z where H_{lr} becomes maximum.* We define this position as $Z_{\max}$. However, $Z_{\max}$ cannot be defined in the case that $H_{lr} = 0$.

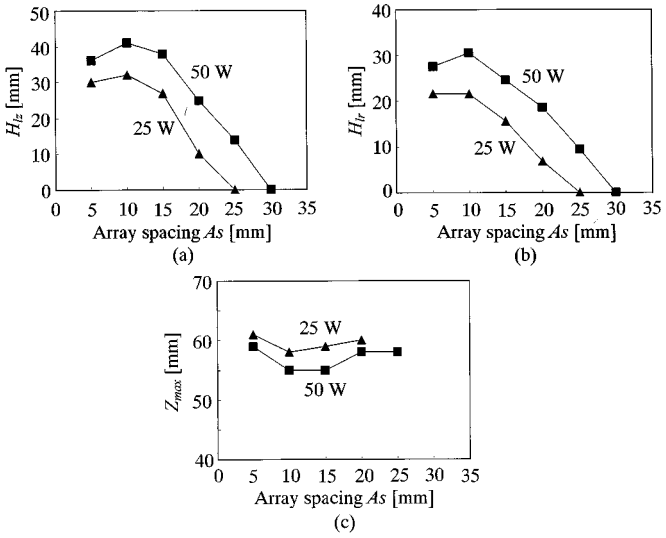

Fig. 9. Heating performances of two-antenna array applicator. (a) Dependence of H_{lz} on As. (b) Dependence of H_{lr} on As. (c) Dependence of $Z_{\max}$ on As.

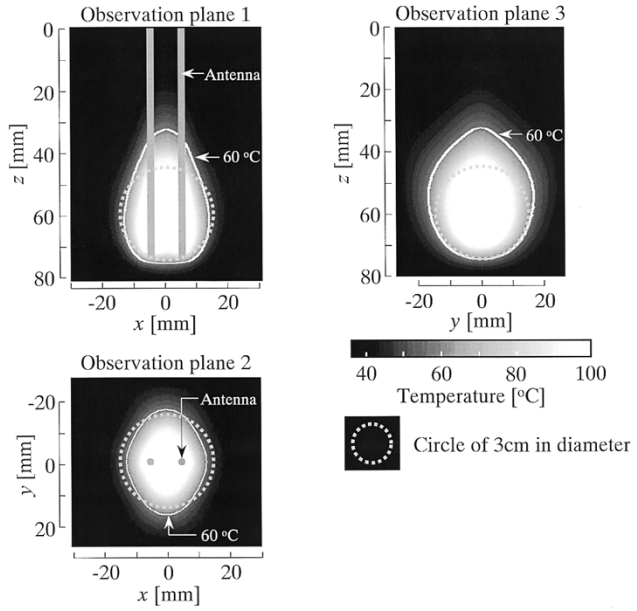

Fig. 10. Temperature distributions of two-antenna array applicator ($As = 10$ mm, $P_{\rm net} = 50$ W).

Fig. 9 shows the calculated results. Fig. 9(a) and (b) shows the indexes H_{lz} and H_{lr}, respectively, for the array spacing As over the range of 5–30 mm. Fig. 9(c) shows the index $Z_{\max}$ where H_{lr} becomes maximum for array spacing As over the range of 5–25 mm. From Fig. 9(a), the index H_{lz} becomes maximum at $As = 10$ mm, for both values of $P_{\rm net}$.

In Fig. 9(b), the index H_{lr} decreases monotonously with increasing values of As over the range of 5–30 mm when $P_{\rm net} = 25$ W. However, the index H_{lr} has the peak value at $As = 10$ mm when $P_{\rm net} = 50$ W. The index $H_{lr} = 0$ when $As = 25$ mm and $P_{\rm net} = 25$ W or when $As = 30$ mm and $P_{\rm net} = 50$ W. Therefore, we may consider that each element of the array applicator became independent of these array spacings.

When $Z_{\max}$ is small, the effective heating around the tip of the antenna is impossible. However, from Fig. 9(c), $Z_{\max}$ takes almost constant values between 55–60 mm at both values of P_{net} for As over the range of 5–25 mm. From this result, we find that two-antenna array applicator can generate the effective heating region around the tip.

We introduced the array applicators to expand the coagulated region in the perpendicular direction of the antenna. Fig. 10 shows the temperature distributions of the two-antenna array applicator in the observation planes when $As = 10$ mm and $P_{\text{net}} = 50$ W because the index H_{lr} was the largest under this condition. In Fig. 10, the circles of 3 cm in diameter are shown as gray dotted line. From Fig. 10, it is revealed that the size of region of 60 °C or more almost covers the sphere with the diameter of 3 cm. This result clearly shows that the array applicator expands the coagulated region and is useful for the MCT.

VI. Conclusions

The heating performances of the array applicator composed of two coaxial-slot antennas for the MCT have been studied. First, we introduced the FDTD method for the electromagnetic analysis and the FDM for the temperature analysis. The validity of these analyses was confirmed by comparing the calculated results with the experimental results. Next, we employed the array applicator composed of two coaxial-slot antennas to expand the coagulated region because generating the coagulated region with a diameter of 3 cm inside the tissue has been required from the clinical side. As a result, we could obtain the coagulated region whose diameter is approximately 3 cm, when the array spacing was 10 mm and the net input power of each antenna was 50 W. This result means that the use of the array applicator is very useful in the MCT.

As a further study, in order to obtain the larger coagulated region by using the array applicator, we have to optimize the number of antenna elements and improve the structure of each element.

Appendix

The finite-difference approximation can be written as follows:

$$\begin{aligned} T_{ijk}^{n+1} &= \frac{\kappa_{ijk}\Delta t}{\rho_{ijk}c_{ijk}}\Big(C1x_{ijk}T_{i-1jk}^{n}+C3x_{ijk}T_{i+1jk}^{n} \\ &\quad +C1y_{ijk}T_{ij-1k}^{n}+C3y_{ijk}T_{ij+1k}^{n} \\ &\quad +C1z_{ijk}T_{ijk-1}^{n}+C3z_{ijk}T_{ijk+1}^{n}\Big) \\ &\quad +\left\{1-(C2x_{ijk}+C2y_{ijk}+C2z_{ijk})\frac{\kappa_{ijk}\Delta t}{\rho_{ijk}c_{ijk}} \right. \\ &\quad \left. -\frac{\rho_{ijk}\rho_{bijk}c_{bijk}F_{ijk}\Delta t}{\rho_{ijk}c_{ijk}}\right\}T_{ijk}^{n}+\frac{\Delta t}{c_{ijk}}\text{SAR}_{ijk} \end{aligned} \tag{A1}$$

$$C1x_{ijk} = \frac{8}{(\Delta x_{i-1jk}+\Delta x_{ijk})(\Delta x_{i-1jk}+2\Delta x_{ijk}+\Delta x_{i+1jk})} \tag{A2}$$

$$C2x_{ijk} = \frac{8}{(\Delta x_{i-1jk}+\Delta x_{ijk})(\Delta x_{ijk}+\Delta x_{i+1jk})} \tag{A3}$$

$$C3x_{ijk} = \frac{8}{(\Delta x_{ijk}+\Delta x_{i+1jk})(\Delta x_{i-1jk}+2\Delta x_{ijk}+\Delta x_{i+1jk})}. \tag{A4}$$

Here, for a continuous function of space and time $f(x, y, z, t)$, its discretized form at the nth time step can be written as $f_{ijk}^{n} = f(i\Delta x, j\Delta y, k\Delta z, n\Delta t)$, where Δx, Δy, and Δz are cell sizes in the finite-difference representation and Δt is the incremental time step. Other coefficients $C1y_{ijk}$, $C2y_{ijk}$, $C3y_{ijk}$, $C1z_{ijk}$, $C2z_{ijk}$, and $C3z_{ijk}$ in (A1) are given by replacing x in (A2)–(A4) with y and z.

References

[1] T. Seki, M. Wakabayashi, T. Nakagawa, T. Itoh, T. Shiro, K. Kunieda, M. Sato, S. Uchiyama, and K. Inoue, "Ultrasonically guided percutaneous microwave coagulation therapy for small carcinoma," *Cancer*, vol. 74, no. 3, pp. 817–825, 1994.

[2] R. Murakami, S. Yoshimatsu, Y Yamashita, T. Matsukawa, M. Takahashi, and K. Sagara, "Treatment of hepatocellular carcinoma: Value of percutaneous microwave coagulation," *Amer. J. Rentgenol.*, vol. 164, pp. 1159–1164, 1995.

[3] T. Shibata, T. Niinobu, T. Murakami, T. Ishida, N. Shibata, and M. Takami, "An experimental study on microwave coagulation in ischemic liver" (in Japanese), *J. Microwave Surgery*, vol. 16, pp. 5–9, 1998.

[4] K. Saito, Y. Hayashi, H. Yoshimura, and K. Ito, "Numerical analysis of thin coaxial antennas for microwave coagulation therapy," in *IEEE Int. AP-S Symp. Dig.*, July 1999, pp. 992–995.

[5] K. Ito, K. Ueno, M. Hyodo, and H. Kasai, "Interstitial applicator composed of coaxial ring slots for microwave hyperthermia," in *IEEE Int. AP-S Symp. Dig.*, Aug. 1989, pp. 253–256.

[6] K. S. Yee, "Numerical solution of initial boundary value problems involving Maxwell's equations in isotropic media," *IEEE Trans. Antennas Propagat.*, vol. AP-14, pp. 302–307, May 1966.

[7] K. Saito, O. Nakayama, L. Hamada, H. Yoshimura, and K. Ito, "Basic study of the coaxial antennas for minimally invasive microwave thermal therapy," in *Proc. IEEE 20th Annu. Int. EMBS Conf.*, Oct. 1998, pp. 3261–3264.

[8] H. H. Pennes, "Analysis of tissue and arterial blood temperatures in the resting human forearm," *J. AppL. Phys.*, vol. 1, pp. 93–122, 1948.

[9] J. Wang and O. Fujiwara, "FDTD computation of temperature rise in the human head for portable telephones," *IEEE Trans. Microwave Theory Tech.*, vol. 47, pp. 1528–1534, Aug. 1999.

[10] F. A. Duck, *Physical Properties of Tissue*. New York: Academic, 1990.

[11] J. Patterson and R. Strang, "The role of blood flow in hyperthermia," *Int. J. Rad. Oncol. Biol. Phys.*, vol. 5, pp. 235–241, 1979.

[12] P. M. Van Den Berg, A. T. De Hoop, A. Segal, and N. Praagman, "A computational model of the electromagnetic heating of biological tissue with application to hyperthermic cancer therapy," *IEEE Trans. Biomed. Eng.*, vol. BME-30, pp. 797–805, Dec. 1983.

Kazuyuki Saito (S'99) was born in Nagano, Japan, on May 7, 1973. He received the B.E. degree in electrical and electronics engineering and the M.E. degree in electronics and mechanical science from Chiba University, Chiba, Japan, in 1996 and 1998, respectively, and is currently working toward the Ph.D. degree at Chiba University.

Since 2000, he has been a Research Fellow with the Japan Society for the Promotion of Science, Chiba, Japan. His main interest is in the area of medical applications of microwaves, including MCT.

Mr. Saito is a member of the Institute of Electrical, Information and Communication Engineers (IEICE), Japan, and the Japanese Society of Hyperthermic Oncology. He was the recipient of a 1997 IEICE AP-S Freshman Award and the 1999 Young Scientist of the URSI General Assembly Award.

Yoshihiko Hayashi was born in Nagano, Japan, on April 2, 1975. He received the B.E. and M.E. degrees in electrical and electronics engineering from Chiba University, Chiba, Japan, in 1998 and 2000, respectively.

His main interest is in the area of medical applications of microwaves, including MCT. He is currently with the Mitsubishi Electric Corporation, Tokyo, Japan.

Mr. Hayashi is a member of the Institute of Electrical, Information and Communication Engineers (IEICE), Japan, and the Japanese Society of Hyperthermic Oncology.

Hiroyuki Yoshimura (M'00) was born in Hyogo, Japan, in 1965. He received the B.E., M.E. and D.E. degrees from Hokkaido University, Sapporo, Japan, in 1987, 1989 and 1994, respectively, all in electronic engineering.

From 1989 to 1991, he was with the Department of Electronic Technics, Toyota Motor Corporation, Aichi, Japan. From 1994 to 1998, he was a Research Associate at the Research Institute for Electronic Science, Hokkaido University. He is currently an Associate Professor in the Department of Urban Environment Systems, Faculty of Engineering, Chiba University, Chiba, Japan. His research interests include optically controlled antennas, medical application of microwave and light, optical information processing, and optical measurement systems based on coherence theory.

Koichi Ito (M'81) was born in Nagoya, Japan, on June 4, 1950. He received the B.S. and M.S. degrees from Chiba University, Chiba, Japan, in 1974 and 1976, respectively, and the D.E. degree from the Tokyo Institute of Technology, Tokyo, Japan, in 1985, all in electrical engineering.

From 1976 to 1979, he was a Research Associate at the Tokyo Institute of Technology. He was a Research Associate (1979–1989) and an Associate Professor (1989–1997) at Chiba University. He is currently a Professor in the Department of Urban Environment Systems, Faculty of Engineering, Chiba University. In 1989, 1994, and 1998, he was an Invited Professor with the Universite de Rennes I, Rennes, France. His main interests include analysis and design of printed antennas, small antennas, research on the interaction between the electromagnetic fields and the human body, and antennas for medical application of the microwaves.

Prof. Ito is a member of the American Association for the Advancement of Science (AAAS), the Institute of Electrical, Information and Communication Engineers (IEICE), Japan, the Institute of Image Information and Television Engineers of Japan, and the Japanese Society of Hyperthermic Oncology.